International Journal of Modern Agriculture, Volume 9, No.3, 2020
ISSN: 2305-7246

MACHINE LEARNING TECHNIQUES AND HYBRID FEATURE EXTRACTION BASED CT LUNG CANCER CLASSIFICATION

P. Priyadharshini*[1], B. S. E. Zoraida#[2]

[1]Research Scholar, Department of Computer Science and Engineering, Bharathidasan University, Tiruchirappalli, India.

[2]Assistant Professor, Department of Computer Science and Engineering, Bharathidasan University, Tiruchirappalli, India. :
Affiliation

[1]email1 priya.tanusri@gmail.com.

[2]email2 b.s.e.zoraida@gmail.com

Abstract

Finding malignant nodules in the lungs using as medical system of computed tomography (CT) is a difficult and time-consuming task for a radiologist. A computer-aided diagnostic (CAD) system is proposed to alleviate this burden. In recent years, the thorough training approach has proven effective. Better results than classic methods in various areas. Currently, researchers are using various machine learning methods to improve the efficiency of the CAD system in detecting lung cancer using computed tomography. In this work, To improve the CAD based CT lung cancer detection, Hybrid feature extraction techniques is introduced. The hybrid feature extraction is based on three different features such as Local Binary Pattern (LBP), Gray-Level Co-Occurrence Matrix (GLCM) and histogram of oriented gradients (HOG). In order to test the classification accuracy by using three different kind of machine learning methods are used such as Random forest, Decision tree and Artificial neural network. The proposed system has evaluated with the help of online available LIDC-IDRI Dataset CT images. The proposed system performances are validated in the terms of sensitivity (SE), Recall (R), Precision (P), specificity (SP), and accuracy (AC).

Keywords-Gray-Level Co-Occurrence Matrix (GLCM); computed tomography (CT); Local Binary Pattern (LBP); computer-aided diagnosis (CAD); Hybrid feature extraction techniques; histogram of oriented gradients (HOG).

I. INTRODUCTION

With the rapid growth of technology, the majority of people suffering from genetic problems due to false mutations [1] completely change their lifestyle. Wrong mutations completely change the structure and function of DNA. Falsely modified DNA cells cause abnormal growth of DNA cells instead of old DNA cells. Abnormal mutations [2] are caused by many external factors, such as breathing of the population through the respiratory tract, alcohol consumption, exposure to chemical gases and so on. Most often, abnormal cell (DNA) mutations [3] lead to tumors that can appear anywhere in the human body, such as the lungs, skin, breasts and brain. Of the various cancers, lung cancer [4] is the most serious disease affecting the respiratory system due to external factors. According to a 2005 study, the death toll rose to 159,292, up from 25% in 2018. A report from the American Association for Central Cancer Registries [5] states that 234,130 people were diagnosed with lung cancer in year of 2018.

In addition, the American Cancer Society surveyed in the United States in 2019 [6] that 228,150 new people were diagnosed with lung cancer, 111,710 women and 116,440 men. According to the analysis, 142,671 persons died from lung cancer. Finally, following the results of the survey, it was decided that the proportion of people suffering from lung cancer has gradually increased over the years. According to the analysis, lung tumor is one of the most public diseases deliberated in medicine for early diagnosis [7]. Lung cancer is self-diagnosed by symptoms such as cough, shortness of breath, fatigue, chest pain, weight loss, memory loss, broken bones, joint pain, and headache. After the patient was affected by the technology, various diagnostic procedures were routinely used to diagnose neurological problems, bleeding, facial swelling, voice changes, and sputum pigmentation. [8-9]. Based on the screening methods, the National Institutes of Health and Public Health provide general guidelines for effective diagnosis of cancer and the stage of lung cancer.

Effective methods for detecting lung cells and cellular lesions are used to foretell lung cancer, but it is difficult to maintain the accuracy of this prediction. Among the selection methods, computed tomography [10] is

International Journal of Modern Agriculture, Volume 9, No.3, 2020
ISSN: 2305-7246

an operative screening method that effectively scans abnormalities and changes in the human body, noticed by X-rays on the human body. Internal organ function is successfully monitored using a 30-minute X-ray, and tissue and lesion details are together efficiently associated to PET and MRI. Based on computed tomography, an automated lung cancer scoring system [11] is being developed to detect disease using a number of traditional steps, such as noise detection, scoping, cancer sign detection, feature selection and cancer classification [12]. Based on the steps described, the process of segmentation and isolation of the target area plays an important role, as the area successfully predicts changes in normal and cancerous cells.

In addition, the divided part helps to shed light on the important symptoms of cancer, thereby reducing the difficulty of the system. Thus, the feature selection procedure [13] reduces the counting time to predict cancer and also decreases the likelihood of data fit. There are various methods of segmentation [13] such as clustering, distributed clustering, hard edge detection, obscure C-instrument, obscure K-means clustering, self-organized maps and neural networks. Hopfield is used to isolate critical areas of X-ray imageries. Different properties are then obtained from the selected area and the optimal properties are selected using different selection methods [15], e.g. B. Packaging approaches, ant colony approaches, genetic algorithms, fireflies and swarms of bacteria that are used to select real functions. Go. From a number of functions. By selecting the features of these selected lung cancers, K-proximal, SVM, and other intelligent classifications were performed. Although traditional automated systems have successfully predicted lung cancer, they provide identification accuracy [16] and take longer to process large amounts of data. In addition, the scheme cannot process the lowest quality CT images, which can lead to improper functioning and classification of the lungs [17]. Then different authors commented on the process of detecting lung cancer because their cancer will help to understand the idea of developing a smart cancer prognosis system.

II. RELATEDWORKS

Kalra, Aggarwal and Furquan [18] has anticipated a model that allows for the classification of nodules and usual lung anatomy. The technique draws geometric, statistical and grayscale features. LDA is used as the optimal threshold for classifier and segmentation. The accuracy of the system is 84%, the sensitivity is 97.14% and the specificity is 53.33%. Although the scheme detects a dangerous lump, its accuracy is unacceptable. There is no machine learning approaches are used for classification, simple segmentation methods are used. Therefore, there is no room for development in our new model by integrating any of its steps.

Jin, Jin and Zhang [19] He used the offensive neural network as a classifier in his CAD scheme to detect LC. The accuracy of the system is 84.6%, a sensitivity is 82.7% and specificity is 86.7%. This model benefits is that it uses filters to get information about that area and area of interest (ROI), reducing costs between training and identification phases. Although the cost of implementation has been reduced, the accuracy is unsatisfactory..

Govindaraju and Sangamithraa [20] uses K unsustainable learning algorithm for grouping or segmentation. Pixel set groups based on certain characteristics. This model applies retro propagation networks for their classification. Traits such as entropy, correlation, homogeneity, PSNR, SSIM are removed using the GLCM method. The accuracy of the system is about 90.7%. Image preprocessing media filters are used for tone extraction. This could be useful for our new model to improve clay extraction and accuracy.

Hou et al. [21] recommended a automatic encoder for core detection and feature extraction. The method integrates core sensing and feature learning in a solo network. The network encodes the cores into subtle feature maps that indicate the locations and appearance of the cores and can be fine-tuned for continuous supervised learning.

Senthil Kumar K et.al [22] has various optimization algorithms are used to detect lung cancer using computed tomography procedures. During the examination, Process 5 methods include a clustering, medium clustering and particle swarm optimization approach to examine tumors on the CT image of the lung. The sound in the recorded CT image is extracted using an adaptive medium filter and histogram analysis is smeared to enhance the image. The various features are then removed and the precious areas are identified using the above algorithm. Thus, the system presented by the author effectively detects up to 95.89% of lung cancer patient.

III. PROPOSED SYSTEM

In this research study, we proposed the method to predict the lung cancer diseases in earlier stage. In below figure 1 exposed the proposed architecture of lung cancer prediction method using machine learning algorithm. Primary the input image is initially preprocess to enhance the image by removing the unwanted noise from input image. Then the preprocessed images is given to the DWT-GLCM, HOG and LBP technique of feature extraction. After FCM technique used to segment the image. Finally, the segmented images is given to the classification machine learning of different three algorithm such as RF, DT and ANN model. This model classify the lung images as normal or tumor.

International Journal of Modern Agriculture, Volume 9, No.3, 2020
ISSN: 2305-7246

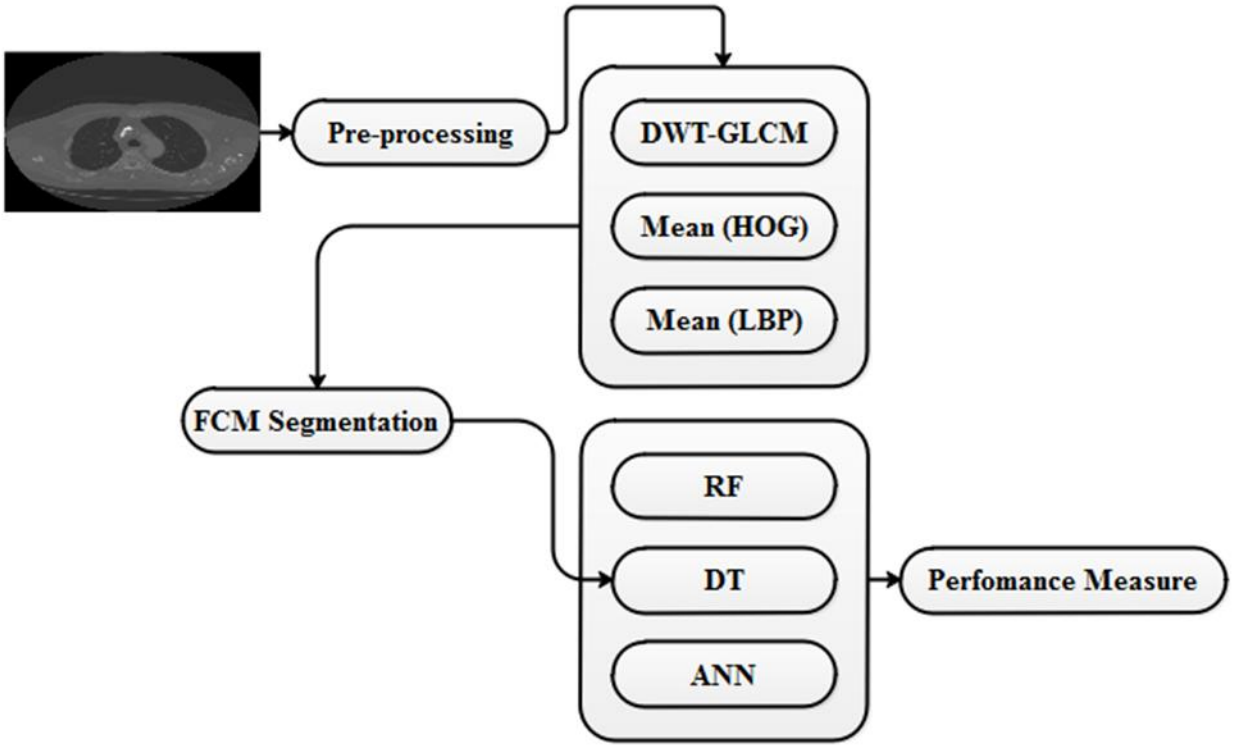

Figure 1: Proposed flow diagram.

A. Pre-processing

In this work for pre-processing process Digital Gaussian filter is used. The Gaussian filter can be stated as:.

$$G(x, y) = \frac{1}{\sqrt{2\pi\sigma}} exp(-x^2 + y^2)/2\sigma^2 \tag{1}$$

Where σ^2 is the variance of Gaussion filter. And the size of the filter kernel $I(-l \leq x, y \leq l)$ is often resolute by neglecting values lower than five presernt of the extreme value of the kernal. The preprocessed imageries are assumed to the Feature extraction unit.

B. Segmentation

The Fuzzy-C-Mean-Clustering-Algorithm (FCM) is an iterative clustering technique that produces an optimal C-division by minimalizing the objective quadratic error function by minimalizing the sum of the JFCM group. [23]:

$$J_{FCM} = \sum_{k=1}^{n} \sum_{i=1}^{c} (u_{ik})^q \, d^2(x_k, v_i) \tag{2}$$

Where u_{ik} is the membership degree of x_k in the i^{th} cluster, $d^2(x_k, v_i)$ is a distance amount among object x_k, q is a weighting exponent on each fuzzy membership, vi is the prototype of the cluster Centre$i$, and cluster centrev_i. A object solution function J_{FCM} can be gotten via an iterative procedure, which is approved out as follows:

1. Fixed value for c, q and $\in$.
2. Initialize the fuzzy matrix $U = [u_{ik}]$.
3. Fixed the loop counter $m = 0$.

4. Compute the c cluster center $\{v_i^{(m)}\}$ with $U^{(m)}$:

$$v_i^{(m)} = \frac{\sum_{k=1}^{n}(u_{ik}^{(b)})^q\, xk}{\sum_{k=1}^{n}(u_{ik}^{(b)})^q} \quad (3)$$

5. Compute the membership$U^{(b+1)}$. For $k = 1$ to n, compute the subsequent: $I_k = \{i|1 \le i \le c, d_{ik} = \|x_k - v_i\| = 0\}$ I:
   (a) If $I_k = \emptyset$ then

$$u_{ik}^{(m+1)} = \frac{1}{\sum_{j=1}^{c}(\frac{d_{jk}}{d_{jk}})^{\frac{2}{(q-1)}}} \quad (4)$$

   (b) Else $u_{ik}^{(m+1)} = 0$ for all $i \notin I$ and $\sum_{i \in I_k} u_{ik}^{(m+1)} = 1$;next k.
6. If $||U^{(m)} - U^{(m+1)} < \in$, stop; otherwise, set $m = m + 1$ and go to phase 4.

C. Feature extraction

To calculate the input coefficient of the segmented images, Discrete Wavelet Transform (DWT) is used, which takes into account the rectangular function. The DWT system has excellent energy compression, short assist filters, low computation and correct reconstruction without redundancy. DWT follows an ambiguous noise procedure, which provides better directional selectivity, with sub-bands that can change and lower frequency. In the multi-resolution process, the actual image composition is calculated by magnification and subtraction. In general, images are broken down into multiple sub-images at various resolution stages to keep the information low and high frequency. The DWT property helps you extract information about textures from images. The squared integral function f(u) and the wave transformation w represent the internal product f, and the value ψ(u) is the function of the real value. The wave function is given in (5).

$$w[f(s,\tau)] = \left(f, \psi_{s,t}^k\right) = \int_{\infty}^{\infty} f(u)\psi_{s,t}^k\,(u)du \quad (5)$$

$$Where, \psi_{s,t}^k(u) = \left(\frac{1}{\sqrt{s\psi_{s,t}^k}}/s\right) denotes \quad (6)$$

. Wave family, $s \epsilon z$ is scale, τ is translation and $k \in \{h, v, d\}$is orientation parameters. These have h, v and $d$denote vertical, horizontal and diagonal direction respectively. The DWT achieved during$s = 2^j$ and $\tau = 2^j, n, j, n\varepsilon z$. the dyadic wavelet is a scalable trial of DWT; it trails a geometric sequence of ratio 2. The resulting wavelet decomposition employs dyadic wavelets that are applied using perfect reconstruction filter banks. By using wavelet function $\psi(u)$ and the scaling function $\varphi(u)$, which showed in Eq. (7) and (8). The wavelet atoms describe by scaling and three mother atomsψ^h, $\psi^v$and ψ^d. This mother atoms considered as the tensor products of 1-D $\psi(u)$and$\varphi(u)$, that is denoted in (7) and (8).

$$\psi_{j,n}^k(u) = \frac{1}{\sqrt{2^j}}\psi^k(\frac{u-2^j.n}{2^j}) \quad (7)$$

$$\varphi_{j,n}^k(u) = \frac{1}{\sqrt{2^j}}\psi^k(\frac{u-2^j.n}{2^j}) \quad (8)$$

$$\varphi(u) = \varphi(u_1)\varphi(u_2), \psi^k(u) \quad (9)$$

The 2-D DWT is implemented with a grouping of down-samplers and digital filter sets. The digital filter bank contains of a low-pass filter and a high-pass filter. The bank number is grouped according to the desired functions in the wavelet configuration structure. Further, the rows and columns of leaf disease images are separately processed by the one-dimensional wavelet transform to create a 2-D wavelet coefficient. The unique images A_ (2 ^ (j + 1)) with full resolution 2 ^ (j + 1) are decomposed into images with 4 sub bands in the frequency domain. Three sub-band images such as$D_{2^i}^h f, D_{2^i}^h f$ *and* $D_{2^i}^h f$ are the original images in resolution between the 4-subband images in vertical, horizontal and diagonal. The 4th image is an approximation image, $A_{2^i}f$ found at coarse resolution, so the entire leaf diseases image $A_{2^{j+1}}f$ is denoted in the (10).

$$A_{2^{j+1}}f = D_{2^i}^h f, +D_{2^i}^v f + D_{2^i}^d f + A_{2^i}f \quad (10)$$

The sub-images are the 2-D orthogonal wavelet. The results of the wavelet decomposition of an image is 4-orthogonal sub-bands such as Low-Low (LL) band, High-Low (HL) band Low-High (LH) band, and High-High (HH) band, which is represented as $D^h_{2^i}f, +D^v_{2^i}f + D^d_{2^i}f and A_{2^i}f$ respectively.In this effort, the fundamental phase of the constituent extraction is LL wavelet highlights are extricated from each splitfilms, using the wavelet illumination, a matrix of concomitant gray level events is applied, and the element estimates fade out. Registers such as autocorrelation, contrast, correlation, correlation, cluster output, cluster hue, difference, energy entropy, uniformity, uniformity, extreme likelihood, number of cubes, variance, normal sum, and sum change, entropy of a sum, difference fluctuation, and entropy conversion are highlighted. , the evidence of correlation1, the informational proportion of correlation2, the inverse difference, the standardized inverse contrast and the normalized inverse of the change [24]. Additionally, sum of HOG features and sum of LBP features are extracted from the segmented image. The HOG, LBP features are cascaded with the DWT, GLCM features. The combined features are used for training and testing for the machine learning network.

D. *Classification*

In this proposed system three different kind of Classification techniques are used such as Random forest, Decision tree and Artificial neural network, Which are detailed in the below section.

Random forest: RF is a tree based technique that is utilized for both organization and relapse inspection. Different trees are developed and the mean forecast would be the return for combination.

Decision tree: DT is an attitude to displaying info. Use a tree drawing as a forecasting model. The goal of the DT is to create a perfect to predict results or values based on input factors. The results represent an important sequence and are widely used for simple orientation. This technique is a well-known artificial intelligence tool that can aid you find the right process for achieving stunning resolutions, because it can be converted into many important criteria by integrating path concentrators and final concentrators.

Artificial neural network: In fact, RNA is thought to be in the neural network that resides in the human brain. ANN works with the hidden state. These dormant states are like neurons. Each of these latent states is a transitional type that exhibits potential behavior. The grid of this dormant state acts as a bridge between the entrance and the exit. Input level, i.e. the data provided by ANN. Hidden layers where there was magic. Finally, the output layer, which contains the final network calculation.

IV. Results and Discussion

The proposed system was tested with a 3.0 GHz Intel i3 Matlab processor (version 2018a), a 1 TB hard drive and 8 GB of RAM. In order to determine the efficacy of the project system, it is associated with the existing system in the LIDC-IDRI data set. It is a trusted online resource that enables PCs to identify and draw conclusions about lung injuries, and to create and design demonstrations (CAD). To collect this information, 10 scientists worked together and set up eight restoration institutes with 1,018 cases. Each subject combines images from the clinical breast CT scan and the associated XML archive and records the final BOF image reported by four experienced chest radiographers.

A. *Evaluation Metrics*

Challenge score metrics are used to appraise the collective presentation and ranking of our method. The assessment criteria for classification accuracy (AC), jacquard index (JSI), and solids coefficient classification (DSC) include sensitivity (SE), specificity (SP), and accuracy (AC). Performance criteria are defined as follows:

$$SE = \frac{tp}{tp+fn} \tag{11}$$

$$SP = \frac{tn}{tn+fp} \tag{12}$$

$$\mathrm{AC} = \frac{tp+tn}{tp+fp+tn+fn} \tag{13}$$

Where tp, tn, fp and fn signify the amount of a true positive, false positive, true negative, and false negative.

B. *Performance Evaluation*

Table 1: classification performance measures

Technique	SE	SP	P	R

International Journal of Modern Agriculture, Volume 9, No.3, 2020
ISSN: 2305-7246

RF	61.44	98.65	91.00	67.25
DT	83.14	89.44	44.38	85.17
ANN	42.86	85.71	60.00	42.86

In table 1 and figure 2 represent the classification of lung cancer performance evaluation of four parameter using three different machine learning algorithm. In RF attained the SE value of 61.44%, SP value of 98.65% and recall value of 67.25%. Another technique of DT attained the SE value of 83.14% and precision of 44.38% and recall value of 42.86%. Next ANN attained the SE value of 42.86%, SP value of 85.71% and recall value of 42.86%.

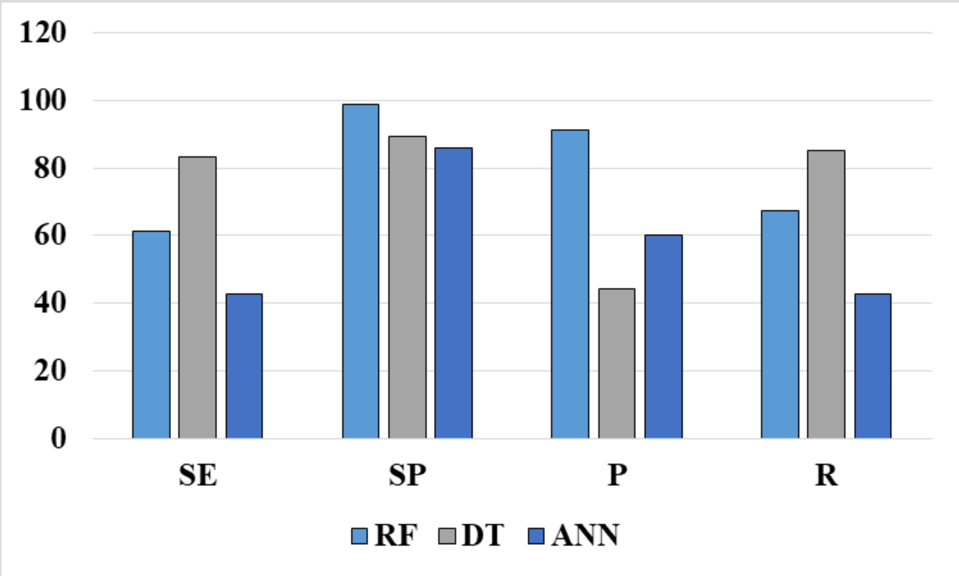

Figure 2: Graphical representation of performance measure

C. Accuracy Analysis

In figure 3 represent the graphical representation of classification accuracy performance. In RF algorithm attained he classification accuracy of 75.14%, DT algorithm attained the accuracy of 77.43%. Another ANN algorithm attained the accuracy of 84.44%. In this comparison analysis's of different three algorithm state that the ANN deliver the better classification accuracy than another two algorithms.

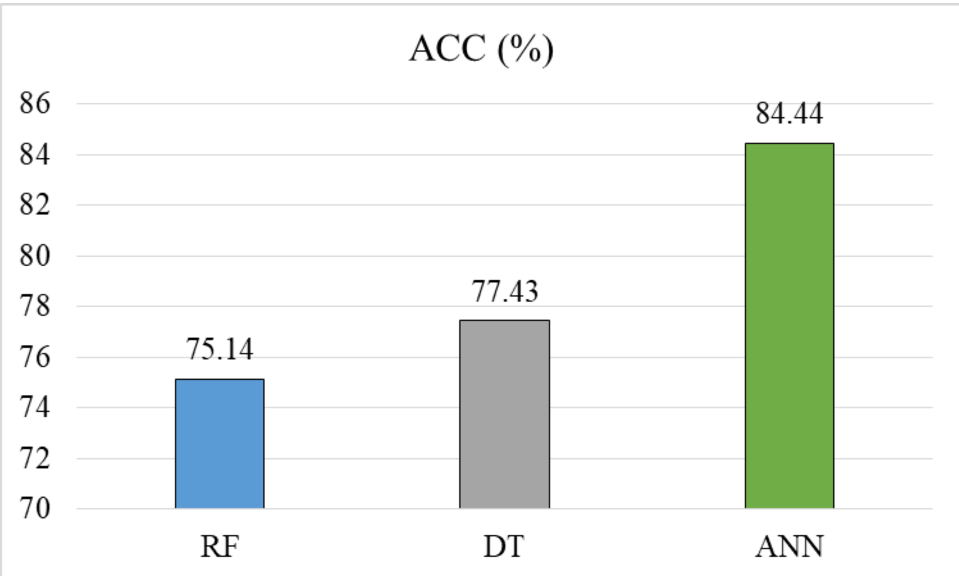

Figure 3: Graphical representation of accuracy measure

V. CONCLUSION

In this dissertation, we have presented various detailed CAD methods and models that share a common goal of making it easier for radiologists to find pulmonary nodules. Compare best performing planning for available datasets using alike metrics can help with their comparative analysis. He shows that machine learning has reached a level of accuracy that allows it to be used not only as a second opinion in analysis, but also as a powerful tool that doctors can evaluate in the course of their work. The presentation of the scheme is estimated based on the outcomes of experiments and the system detects cancer with maximum accuracy. After all, one of the current constraints is data and inequality. In the future, the proposed hybrid feature extraction system will take into account deep learning methods.

REFERENCES

[1] Hong Y, Hong SH, Oh YM,“Identification of lung cancer specific differentially methylated regions using genomewide DNA methylation study”, Mol Cell Toxicol pp. 14:315, 2018. https:// doi.org/10.1007/s13273-018-0034-0

[2] Nair SS et al Comparison of methyl-DNA immunoprecipitation (MeDIP) and methyl-CpG binding domain (MBD) protein capture for genome-wide DNA methylation analysis reveal CpGsequence coverage bias. Epigenetics vol. 6, pp. 34–44, 2011.

[3] Gaudet F et al (2003) Induction of tumors in mice by genomic hypomethylation. Science 300:489–492

[4] Tang M, Xu W, Wang Q, Xiao W, Xu R,“Potential of DNMT and its epigenetic regulation for lung cancer therapy”, Curr Genomics vol. 10, pp. 336–352, 2009.

[5] Liu Z, Wang J, Yuan Z, Zhang B, Gong L, Zhao L, Wang P, “Preliminary results about application of intensity-modulated radiotherapy to reduce prophylactic radiation dose in limited-stage small cell lung cancer”, J Cancer vol. 9, no. 15, pp. 2625–2630, 2018. https://doi.org/10.7150/jca.24976

[6] Balmelli C, Railic N, Siano M, Feuerlein K, Cathomas R, Cristina V, Gu¨thner C, Zimmermann S, Weidner S, Pless M, Stenner F, Rothschild SI, ‘‘Lenvatinib in advanced radioiodine-refractory thyroid cancer: a retrospective analysis of the swiss lenvatinib named patient program. J Cancer vol. 9, no. 2, pp.250–255, 2018, https://doi.org/10.7150/jca.22318

[7] Manser R, Lethaby A, Irving LB, Stone C, Byrnes G, Abramson MJ, Campbell D,“Screening for lung cancer. Cochrane Database of System”,vol. 6, pp. 6, 2013, CD001991. https://doi.org/10.1002/ 14651858.cd001991.pub3

[8] Brock MV et al, DNA methylation markers and early recurrence in stage I lung cancer. N Engl J Med vol. 358, pp. 1118–1128, 2008.

[9] Wang CC et al HOXA5 inhibits metastasis via regulating cytoskeletal remodelling and associates with prolonged survival in non-small-cell lung carcinoma. PLoS ONE vol. 10, pp. 012-411, 2015.

[10] Hulbert A, Jusue-Torres, I, Stark A, Chen C, Rodgers K, Lee B, Belinsky SA,“Early detection of lung cancer using DNA promoter hypermethylation in plasma and sputum”, Clin Cancer Res vol. 23, no. 8, 2017.

[11] Lee HY et al Differential expression of microRNAs and their target genes in non-small-cell lung cancer. Mol Med Rep vol.11, pp. 2034–2040, 2015.

[12] Manogaran G, Shakeel PM, Hassanein AS, Priyan MK, Gokulnath C Machine-learning approach based gamma distribution for brain abnormalities detection and data sample imbalance analysis. IEEE Access, vol.17, pp.12-21, 2018, https://doi.org/10.1109/ ACCESS.2018.2878276

[13] Shakeel PM, Tolba A, Al-Makhadmeh Z, Jaber MM,“Automatic detection of lung cancer from biomedical data set using discrete AdaBoost optimized ensemble learning generalized neural networks”, Neural Comput Appl,vol.17, no. 23, 2019 https://doi.org/10.1007/s00521-018-03972-2

[14] Gambino O, Conti V, Galdino S, Fabio Valenti C, dos Santos WP (2019) Image segmentation techniques for healthcare systems. J Healthc Eng 2019, https://doi.org/10.1155/2019/ 2723419

[15] Pratiwi AI, Adiwijaya,"On the feature selection and classification based on information gain for document sentiment analysis", Appl Comput Intell Soft Comput 2018:1407817. https:// doi.org/10.1155/2018/1407817

[16] Sridhar KP, Baskar S, Shakeel PM, Dhulipala VS, "Developing brain abnormality recognize system using multi-objective pattern producing neural network", J Ambient Intell Humaniz Comput, 2018, https://doi.org/10.1007/s12652-018-1058-y

[17] Shakeel PM, Tobely TEE, Al-Feel H, Manogaran G, Baskar S,"Neural network based brain tumor detection using wireless infrared imaging sensor", 2019, IEEE Access 7:5577–5588.

[18] Aggarwal, T., Furqan, A., & Kalra, K. "Feature extraction and LDA based classification of lung nodules in chest CT scan images." 2015 International Conference On Advances In Computing, Communications And Informatics (ICACCI), 2015, DOI: 10.1109/ICACCI.2015.7275773.

[19] Jin, X., Zhang, Y., & Jin, Q. "Pulmonary Nodule Detection Based on CT Images Using Convolution Neural Network." 2016 9Th International Symposium On Computational Intelligence And Design (ISCID), 2016 DOI: 10.1109/ISCID.2016.1053.

[20] Sangamithraa, P., & Govindaraju, S, "Lung tumour detection and classification using EK-Mean clustering." 2016 International Conference On Wireless Communications, Signal Processing And Networking (Wispnet), 2016, DOI: 10.1109/WiSPNET.2016.7566533.

[21] Hou, L., Nguyen, V., Kanevsky, A. B., Samaras, D., Kurc, T. M., Zhao, T., et al. (2019b). Sparse autoencoder for unsupervised nucleus detection and representation in histopathology images. Pattern Recogn, vol. 86, pp. 188–200, 2019, doi: 10. 1016/j.patcog.2018.09.007

[22] Senthil Kumar K, Venkatalakshmi K, Karthikeyan K,"Lung cancer detection using image segmentation by means of various evolutionary algorithm",2019, Comput Math Methods Med 2019:4909846.

[23] Li K., Cao Z., Cao L., Liu M,"An Improved FCM Algorithm for Image Segmentation", In: Yu J., Greco S., Lingras P., Wang G., Skowron A. (eds) Rough Set and Knowledge Technology, Lecture Notes in Computer Science, vol 6401, 2017.

[24] D A. Clausi, "An analysis of co-occurrence texture statistics as a function of grey level quantization", Can. J. Remote Sensing, vol. 28, no. 1, pp. 45-62, 2002.